



Review

# The role of bulk oxide ion in the catalytic oxidation reaction over metal oxide catalyst

Yoshihiko Moro-oka<sup>a,\*</sup>, Wataru Ueda<sup>b,1</sup>, Kang-Hee Lee<sup>c</sup>

<sup>a</sup> *Tokiwa University, Miwa 1-430-1, Mito, Ibaraki 310-8585, Japan*

<sup>b</sup> *Catalysis Research Center, Hokkaido University, N-11, W-10, Kita-ku, Sapporo 060-0811, Japan*

<sup>c</sup> *Clean Technology Research Center, KIST, P.O. Box 131, Cheongryang, Seoul, South Korea*

Received 12 September 2002; received in revised form 30 October 2002; accepted 30 October 2002

## Abstract

Participation of bulk oxide ion into the catalytic oxidation over metal oxide catalyst is summarized and its concept is discussed in this review. Rapid migration of oxide ion is realized through diffusion depending on the defect structure of metal oxide catalyst. The bulk of oxide catalyst plays an important role in the catalytic oxidation as the bank of active oxygen species and the bank function of the bulk of metal oxide catalyst with the rapid migration of oxide ion enhances both catalytic activity and catalyst life. Two typical examples to design excellent practical oxidation catalyst are introduced for the selective oxidation of olefin and effective automobile catalyst.

© 2003 Elsevier Science B.V. All rights reserved.

*Keywords:* Selective oxidation; Metal oxide catalysts; Catalytic function

## 1. Introduction

The key elementary step of catalytic reaction over heterogeneous catalyst has been specified as the surface reaction between two adsorbed species or direct attack of gaseous molecule to the adsorbed species. Typical reaction modes such as Langmuir–Hinshellwood mechanism and Twigg–Redeal mechanism have been well established, where catalytic reaction consists of continuous steps including the adsorption of reactant molecules, migration of adsorbed species, a series of surface reactions and desorption of the reaction products. However, it has been

sometimes reported that atomic species in the bulk of catalyst are dynamically involved in the catalytic reaction, especially catalytic oxidation over the metal oxide catalysts. The involvement of lattice oxide ion in several metal oxide catalysts into the surface reaction has been implicitly perceived through the rate equation based on the Mars and van Krevelen mechanism [1] where not only the surface oxide ions but also the whole oxide ions in the bulk of catalyst are equally counted as the active species of oxygen for the steady state catalytic reaction.

Clear evidence for the participation of the lattice oxide ion into the catalytic reaction was demonstrated by Keulks and coworkers using <sup>18</sup>O<sub>2</sub> tracer in the oxidation of propylene to acrolein over bismuth molybdate catalyst [2–4]. It was found that lattice oxide ion is predominantly incorporated into the reaction products. Since the catalytic oxidation of olefin has been

\* Corresponding author.

E-mail address: [ueda@cat.hokudai.ac.jp](mailto:ueda@cat.hokudai.ac.jp) (W. Ueda).

<sup>1</sup> Co-corresponding author. Tel.: +81-11-706-2907; fax: +81-11-709-4748.

widely employed for the industrial production of oxygenates in petrochemistry, a variety of the metal oxide catalysts have been developed for the industrial oxidations and ammoxidations of lower olefin. Most of them consist of mixed oxide catalysts based on vanadium, molybdenum, tellurium and antimony oxides and the improvement of the catalytic performance of them has been mainly achieved by the functionalization of catalyst systems, where participation of the lattice oxide ion strongly contributes to the enhancement of catalytic activity and the elongation of catalyst life [5]. It was also pointed out that the participation of the lattice oxide ion into the catalytic oxidation demands rapid migration of oxide ion in the bulk of oxide catalyst, which depends on the defect structure of the bulk of oxide catalyst [6]. These concepts have greatly contributed to the working principle how to make excellent oxidation catalysts.

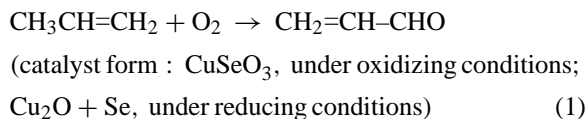
Recently, the concept of the participation of the lattice oxide ion again applied to the design of automobile catalyst by Toyota group. Mixed oxide system having oxygen storage/release function was successfully employed as the co-catalyst of noble metals, where multicomponent metal oxides serve as the bank of active oxygen species [7,8]. This review summarizes the role of the bulk oxide ion of catalyst in catalytic oxidation for the design of excellent oxidation catalyst.

## 2. Catalytic oxidation of lower olefin over metal oxide catalyst

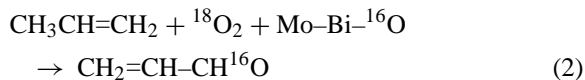
### 2.1. Participation of lattice oxide ion into the reaction

Catalytic oxidation and ammoxidation of lower olefin have been important fundamental processes for petrochemical industry. Oxidation and ammoxidation of propylene have especially investigated to improve catalytic activity and selectivity to form target products. In early stage of the investigation, Kominami studied copper selenide catalyst systems [9]. It was reported that catalyst system took  $\text{CuSeO}_3$  form under the oxidizing conditions and  $\text{Cu}_2\text{O}$  and Se under the reducing conditions during the oxidation reaction of propylene and the oxidation state of the catalyst varies dynamically between two forms depending on

the gas composition. It was estimated that not only the surface species of oxygen but also the oxide ion in the bulk of catalyst take part into the reaction under the steady state reaction conditions.



Both oxidation and ammoxidation of propylene have been widely industrialized after 1959 at which SOHIO established the first industrial process using bismuth molybdate catalyst [10–12]. In 1971, Keulks and coworkers demonstrated the first clear evidence that lattice oxide ion is predominantly incorporated into the reaction products in the oxidation of propylene over bismuth molybdate catalyst using  $^{18}\text{O}_2$  tracer [2–4].



The results mean that the active species of oxygen on the oxide catalyst is in rapid exchange equilibrium with bulk oxide ion or that two different sites are involved in the reaction, one is reaction site and mainly adds active oxygen to the carbon atom to form acrolein and another site exclusively activates gaseous oxygen. The latter case inevitably requires the rapid migration of activated oxygen to the reaction site through the bulk of bismuth molybdate catalyst. It has been known that the bulk migration of oxide ion is accelerated by the formation of lattice vacancies. This may happen in bismuth molybdate catalyst because of its defective structure.

Although the reaction mechanism of the (amm)oxidation of propylene has been precisely investigated and the reaction route from propylene to acrolein or acrylonitrile has been well elucidated [13] but little informations have been reported for the activation of oxygen. A considerable higher rate of oxide ion migration ( $\text{Bi}_2\text{MoO}_6 > \text{Bi}_2\text{Mo}_2\text{O}_9 > \text{Bi}_2\text{Mo}_3\text{O}_{12}$ ) was observed but the participation of lattice oxide ion into the reaction and rapid bulk migration of oxide ion were never correlated with the activity and selectivity of oxidation catalysts including bismuth molybdate in the early stage of the investigations.

## 2.2. Working mechanism of multicomponent bismuth molybdate catalyst

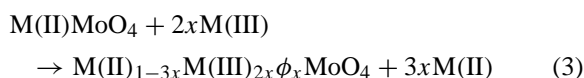
After the establishment of industrial processes, practical catalyst systems for the (amm)oxidation of propylene have been improved year by year. Two types of mixed oxide systems, i.e. multicomponent bismuth molybdate [14–16] and iron antimonite [17] have shown most excellent performance among them. Multicomponent bismuth molybdate has been widely employed in the worldwide industry and shows almost 100 times higher activity than pure bismuth molybdate with keeping excellent selectivity to target products.

In spite of its excellent catalytic activity and selectivity in the industrial oxidation processes, the reason why multicomponent bismuth molybdate catalysts show high-grade performance has not been elucidated. The reaction mechanism to form oxygenates is almost same with simple bismuth molybdate and the structure of the multicomponent catalyst was too much complicated. Several multicomponent oxides having decided composition such as  $\text{Bi}_3\text{FeMo}_2\text{O}_{12}$  [18–20] were proposed as an active component but no clear evidence to support the proposal was presented.

The effort to clarify the high activity and selectivity of multicomponent bismuth molybdate catalysts has been done in our laboratory by using  $^{18}\text{O}$  tracer. It was understood by the resulting lattice vacancies and participation of lattice oxide ion into the catalytic reaction. Almost 100 times enhancement of the catalytic activity of multicomponent bismuth molybdate catalyst based on the 10 times increase of specific surface area and 10 times increase of specific activity compared to the simple bismuth molybdate catalyst [21,22]. Since the specific surface area of simple bismuth molybdates or bismuth phosphomolybdate is not so high (ca.  $1\text{ m}^2/\text{g}$ ), silica gel was usually employed as the support of simple bismuth molybdate catalyst. However, when simple bismuth molybdate is supported on silica gel as thin layer to keep higher specific surface area, it does not show excellent catalytic activity and selectivity for the (amm)oxidation of propylene [23]. Bismuth molybdate was consequently supported on the silica gel as thick layer and the support mainly worked for the strength of mechanical structure of fluidized bed catalyst and not for the enlargement of the specific surface area of bismuth molybdate catalyst.

The practical multicomponent bismuth molybdate catalyst also employed silica as the support but the structure of them other than support is quite complicated. The main part of the catalyst consists of two parts, one is pure bismuth molybdate, i.e.  $\alpha$ ,  $\beta$ , and  $\gamma$  phase of bismuth molybdate and the other is the mixture or solid solution of divalent ( $\text{Co}^{2+}$ ,  $\text{Ni}^{2+}$ ,  $\text{Fe}^{2+}$ ,  $\text{Mn}^{2+}$ ,  $\text{Mg}^{2+}$ ) and trivalent ( $\text{Fe}^{3+}$ ,  $\text{Cr}^{3+}$ ) metal molybdates. It was revealed by surface analysis that the former is located on the surface of the latter as thin layer. Owing to the relatively higher specific surface area of divalent or trivalent metal molybdates ( $5\text{--}10\text{ m}^2/\text{g}$ ), the multicomponent bismuth molybdate has higher specific surface area than simple bismuth molybdate catalyst and this is one of the reasons of the higher activity of the multicomponent bismuth molybdate catalyst.

Another reason is based on the more complicated mechanism. Multicomponent bismuth molybdate catalysts require at least four elements, divalent and trivalent metal cations as well as bismuth and molybdenum, where it is necessary that both divalent and trivalent metal cations have almost the same ionic radius and make solid solution of  $\text{M(II)MoO}_4$  and  $\text{M(III)}_2(\text{MoO}_4)_3$ . It is generally accepted that divalent metal cation and trivalent metal cation are replaced with each other and make cation and anion vacancies in the metal molybdates.



where  $\phi$  means cation vacancy. The replacement of  $\text{M(III)}$  by  $\text{M(II)}$  in  $\text{M(III)}_2(\text{MoO}_4)_3$  may also form anion vacancies. This was confirmed by Ponceblanc et al. in the  $\text{CoMoO}_4\text{--FeMoO}_4$  solid solution system with some amounts of  $\text{Fe}^{3+}$  [24].

The role of lattice oxide ion was clarified using  $^{18}\text{O}$  tracer and model catalyst  $\text{Bi}_2(\text{MoO}_4)_3/\text{Co}_{11/12}\text{Fe}_{1/12}\text{MoO}_4$  by our investigation [21,22]. It was confirmed a part of Fe took trivalent state and some lattice vacancies consequently formed in the bulk of  $\text{Co}_{11/12}\text{Fe}_{1/12}\text{MoO}_4$ . Three kinds of oxygen, i.e. lattice oxide ion in  $\text{Bi}_2(\text{MoO}_4)_3$ , oxide ion in  $\text{Co}_{11/12}\text{Fe}_{1/12}\text{MoO}_4$ , and gaseous oxygen molecule, are available as the source of oxygen atom incorporated into the reaction product in the oxidation of propylene. In order to clarify what kind of oxide ion is incorporated into the reaction product, the reaction was carried out in the reaction

**Mo-Bi-M<sup>II</sup>-M<sup>III</sup>-O**

	Atomic %	Element
Mo <sup>VI</sup>	50~55	
Bi <sup>III</sup>	3~7	
M <sup>II</sup>	30~35	Co, Ni, Fe, Mg, Mn,.....
M <sup>III</sup>	8-15	Fe, Cr, Al, especially Fe
M <sup>I</sup>	small	K, Na, Cs, Tl, ...
X		Sb, Nb, V, W, Te, ...
Y		P, B

Fig. 1. Multicomponent bismuth molybdate catalyst.

system where each source of oxygen was labeled by <sup>18</sup>O. The tracer experiment clearly showed that the oxide ion in Bi<sub>2</sub>(MoO<sub>4</sub>)<sub>3</sub> was first involved in the reaction, then the lattice oxide ion in Co<sub>11/12</sub>Fe<sub>1/12</sub>MoO<sub>4</sub> and in last oxygen atom in gaseous molecule. It was also confirmed that no rapid oxygen equilibrium reactions between different sources of oxygen atom. The results show that the activation of oxygen and the reac-

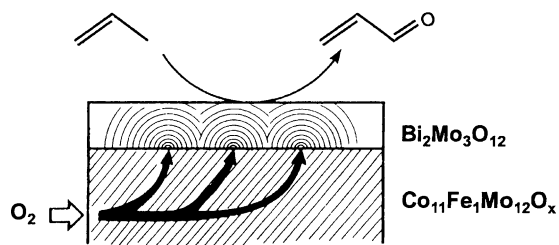


Fig. 2. The scheme of active oxygen migration through the bulk of multicomponent bismuth molybdate catalyst.

tion of propylene take part on the different active sites and oxygen species activated on the separate site from the reaction site migrates through Co<sub>11/12</sub>Fe<sub>1/12</sub>MoO<sub>4</sub> and Bi<sub>2</sub>(MoO<sub>4</sub>)<sub>3</sub> by the bulk diffusion as shown in Figs. 1 and 2.

It was pointed out that this migration is possible only when the catalyst system contains divalent metal cation as well as trivalent metal cation, especially Fe<sup>3+</sup>, with lattice vacancies. The migration of ox-

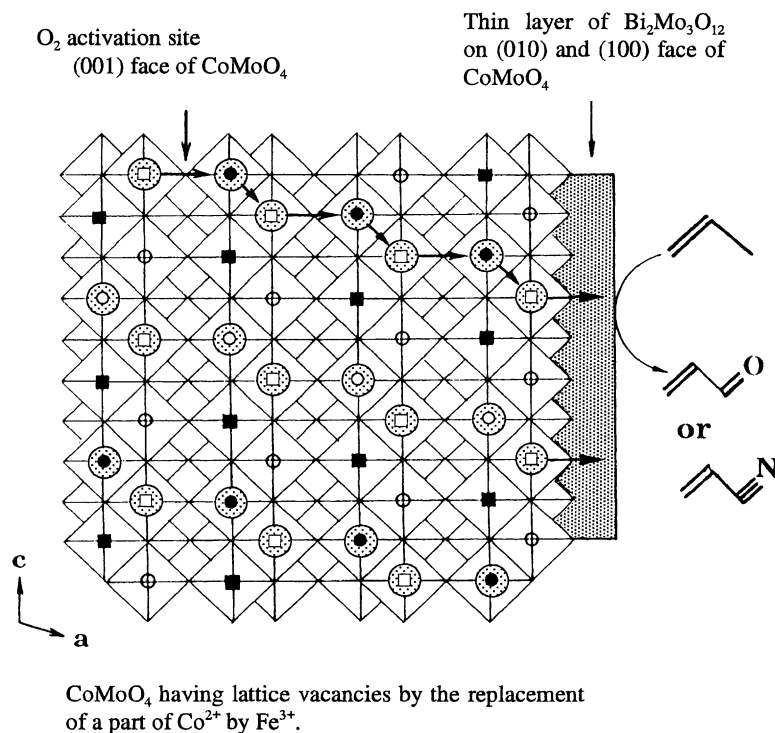


Fig. 3. Active structure model for typical multicomponent bismuth molybdate catalyst.

ide ion consequently accompanies the migration of electron. This functional system also enhances the catalytic activity and increases the number of active reaction site by the smooth supplementation with active oxygen. The estimated functional catalyst system of typical multicomponent bismuth molybdate catalyst, Mo-Bi-Co-Fe-O, is shown in Fig. 3 [25]. The concept described above has been widely utilized for the development of industrial oxidation catalysts.

### 2.3. The enhancement of catalyst life and the design of oxidation catalyst

Industrial catalysts usually require longer catalyst life, which strongly depends on the structural stability of catalyst under the reaction conditions. It was demonstrated that the rapid migration of bulk oxide ion and resulting participation of much amount of bulk oxide ion in the catalytic oxidation enhance the stability of multicomponent metal oxide catalyst [5,26].

The catalyst system having scheelite structure,  $\text{Bi}_{1-x/3}\text{V}_{1-x}\text{Mo}_x\text{O}_4$ , was first reported for the oxidation of propylene by Bierlein and Sleight in 1975 [27]. It was demonstrated that  $\text{V}^{5+}$  cation in  $\text{BiVO}_4$  can be replaced by  $\text{Mo}^{6+}$  until  $x = 0.45$ , forming cation vacancies without changing original scheelite structure. As often reported in the systematic studies of scheelite catalysts by Sleight and coworkers [28–31], catalytic activity to form acrolein and acrylonitrile in the (amm)oxidation of propylene increases drastically with increasing concentration of lattice vacancies in  $\text{Bi}_{1-x/3}\text{V}_{1-x}\text{Mo}_x\text{O}_4$ . The selectivity of propylene oxidation was also improved to some extent with the degree of substitution.

The participation of lattice oxide ion into the oxidation of propylene was investigated by using  $^{18}\text{O}_2$  tracer [5,26]. The oxide ion in the bulk of  $\text{Bi}_{1-x/3}\text{V}_{1-x}\text{Mo}_x\text{O}_4$  catalyst system was clearly involved in the reaction under the steady state conditions, but the degree of participation differed significantly depending on the catalyst composition and resulting concentration of lattice vacancies. It was evaluated by the hypothetical complete mixing volume of lattice oxide ion proposed by Keulks and coworkers [32]. By assuming that the  $^{18}\text{O}$  concentration of bulk oxide ion in the dilution volume of catalyst is equal to that in the oxidized product in the reaction at a given time and  $V$  is the complete mixing volume,  $V$  can be

calculated from the results of  $^{18}\text{O}_2$  tracer experiments:

$$\frac{^{18}\text{O}\% \text{ in products}}{^{18}\text{O}\% \text{ in gaseous oxygen}} = 1 - \exp\left(-\frac{A}{V}\right) \quad (4)$$

where  $A$  is the total amount of molecular oxygen consumed in the reaction until the given time. Eq. (4) is rewritten as

$$\ln\left[1 - \frac{^{18}\text{O}\% \text{ in products}}{^{18}\text{O}\% \text{ in gaseous oxygen}}\right] = -\frac{A}{V} \quad (5)$$

The complete mixing volume calculated by Eq. (5) is the hypothetical volume of catalyst oxide, where lattice oxide ions are under complete equilibrium with surface active oxygen. Accordingly, the larger the volume, the higher the mobility of oxide ion migration and much amount of lattice oxide ions can take part in the reaction.

The fraction of the complete mixing volume to the total amount of lattice oxide ion in the catalyst is

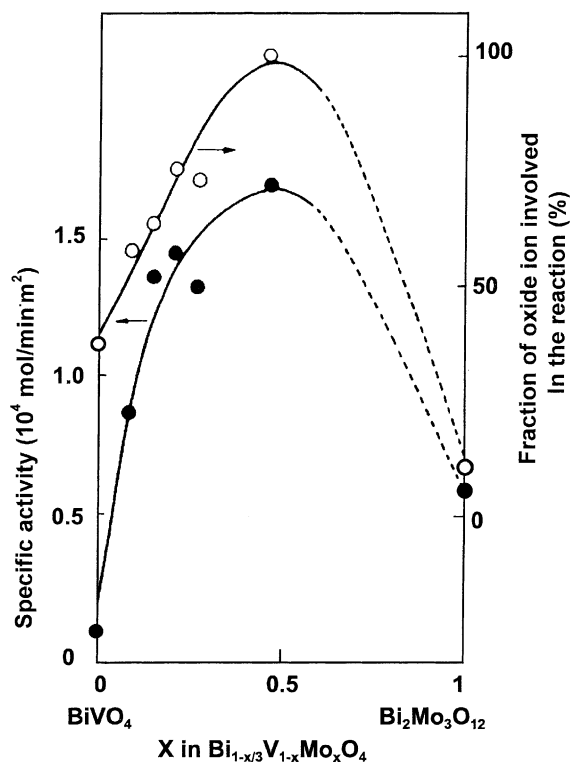


Fig. 4. The specific activity and the fraction of lattice oxide ion involved in the oxidation of propylene over  $\text{Bi}_{1-x/3}\text{V}_{1-x}\text{Mo}_x\text{O}_4$  catalysts.

shown in Fig. 4. The fraction increases with increasing  $x$  until  $x$  reaches 0.45 beyond which the catalyst system can not keep scheelite structure. The variation takes closely the same dependency with that of the specific activity on the catalyst composition. Slight suggested that the increase of the specific activity with the increase of  $x$  came from the increased proton acceptability in the rate-determining abstraction of allylic hydrogen atom of propylene with increasing cation vacancies [5,26]. However, almost the same reaction kinetics (first-order in propylene and zero order in oxygen) and the same apparent activation energy on each catalyst seem rather the increase of active reaction site with the increase of the rate of oxide ion migration.

Clear relationship between the stability of the catalyst system and the migration rate of lattice oxide ion was reported [5]. The stability of the tricomponent catalyst system,  $\text{Bi}_{1-x/3}\text{V}_{1-x}\text{Mo}_x\text{O}_4$ , was examined by the repeated temperature programmed reduction

and reoxidation using XRD. XRD patterns of catalysts at the fresh state, after the reduction to 6% and after the reoxidation are presented in Fig. 5. It is clear that free bismuth metal was detected after the reduction in the XRD patterns of the catalysts having lower molybdenum contents, especially in  $\text{BiVO}_4$ . Free bismuth metal after the reduction decreased with increasing content of molybdenum and no free bismuth metal was detected in  $\text{Bi}_{0.85}\text{V}_{0.55}\text{Mo}_{0.45}\text{O}_4$ , which showed the highest mobility of lattice oxide ion. On the contrary, every peak of fresh catalysts having higher molybdenum concentrations was broadened after the reduction, suggesting the lattice distortion of oxide catalysts by loosening a part of bulk lattice oxide ion homogeneously. The results clearly show that the reduction was localized in the vicinity of the surface but the degree was quite deep in the catalysts having lower molybdenum concentrations. In the cases of higher concentration of molybdenum, the

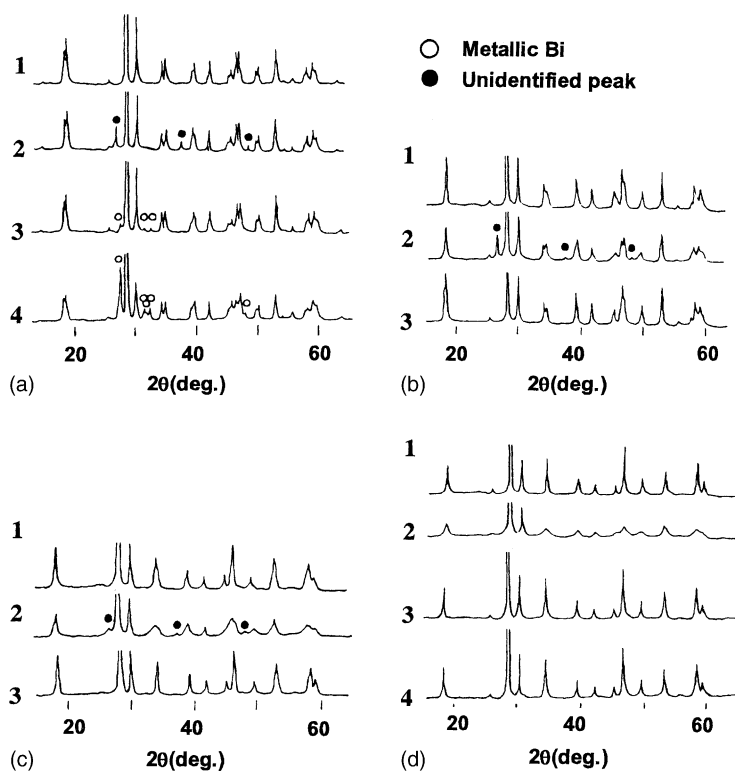


Fig. 5. XRD patterns of the  $\text{Bi}_{1-x/3}\text{V}_{1-x}\text{Mo}_x\text{O}_4$  catalyst systems: (1) at fresh state; (2) after reduction in hydrogen (6%); (3) after TPRO up to 450 °C; (4) after four reduction (450 °C in  $\text{H}_2$ ) and reoxidation (TPRO, up to 450 °C) cycles. (a)  $\text{BiVO}_4$ ; (b)  $\text{Bi}_{0.97}\text{V}_{0.91}\text{Mo}_{0.08}\text{O}_4$ ; (c)  $\text{Bi}_{0.91}\text{V}_{0.73}\text{Mo}_{0.27}\text{O}_4$ ; (d)  $\text{Bi}_{0.85}\text{V}_{0.55}\text{Mo}_{0.45}\text{O}_4$ .

reduction spread to the whole oxide but the catalysts kept their original structures in spite of the lattice distortion by the homogeneous lost of a part of lattice oxide ion. When catalysts were reoxidized in oxygen up to 450 °C, all catalysts recovered their original XRD patterns but some unidentified peaks were observed in the case of  $\text{BiVO}_4$ . After the repeating redox cycles, unidentified peaks in  $\text{BiVO}_4$  grew and the catalyst was decomposed. On the other hand, the catalysts having higher molybdenum concentrations were more stable and their original structures were kept after the repeated redox cycles. Since oxidation catalysts are usually employed under the redox condition and decomposition of complex oxide into each component is the main reason of deactivation, structural stability against the redox cycle is the most important to enhance the catalyst life. The concept is illustrated in Fig. 6.

The thickness of oxide ion layer which may be involved in the catalytic oxidation of propylene under the working conditions was determined by  $^{18}\text{O}_2$  tracer method. As shown in Fig. 7, surface oxide ion involved in the reaction differs significantly depending on the kind of oxide catalyst. Generally speaking, the layer is thin when first transition metal elements, such as Fe, Co, Ni, Mn, Mg, etc. are included as the main

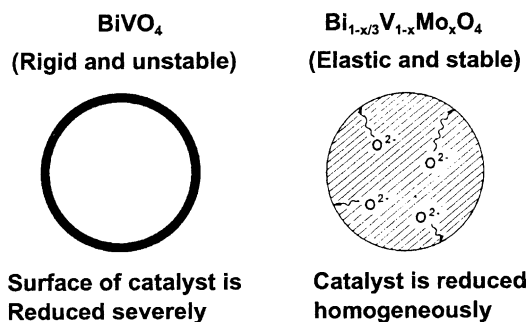


Fig. 6. Concept for the stabilization of multicomponent metal oxide catalyst.

component of active catalyst. It has been well known that these elements are highly active for the activation of molecular oxygen. Thick layer is demanded when catalyst is composed of such element as molybdenum, vanadium, tellurium, bismuth and antimony, which are not so active for the activation of oxygen. Iron–antimony binary oxide catalyst was developed by Nitto Chem. Co. (now, Mitsubishi Layon Co.) for the excellent ammoxidation catalyst for propylene [17]. It has not so thick layer of oxide ion involved in the steady state reaction but it has been improved by the addition of third and fourth elements, molybdenum,

0~1	$\text{Cu}_2\text{O}/\text{Celite}$ $\text{FeSbO}_4$ , $\text{CoMoO}_4$ , $\text{ZnSb}_2\text{O}_6$
10	$\text{Sb}_2\text{O}_4\text{-MoO}_3$ (Sb/Mo = 1/1) $\text{Sb}_2\text{O}_4\text{-TeO}_2$ (Sb/Te = 1/1)
50	$\text{M}_{11}\text{Bi}_1\text{Mo}_{12}\text{O}_x$ (M = Ni, Co, Mg, Mn) $\text{TeO}_2\text{-MoO}_3$ (Te/Mo = 1/1) $\text{CoTeMoO}_6$ , $\text{MnTeMoO}_6$ $\text{Bi}_2(\text{MoO}_4)_3$
100	$\text{Fe-Te-Mo-O}$ $\text{CuO-TeO}_2\text{-6MoO}_3$ $\text{Co}_8\text{Fe}_3\text{Bi}_1\text{Mo}_{12}\text{O}_x$ $\text{Bi}_2\text{MoO}_6$
500	$\text{Pb}_{11}\text{Bi}_1\text{Mo}_{12}\text{O}_x$ $\text{Bi}_{1-x/3}\text{V}_{1-x}\text{Mo}_x\text{O}_4$

Fig. 7. The thickness of oxide ion layer involved in the oxidation of propylene under the working conditions determined by  $^{18}\text{O}_2$  tracer at 450 °C [33].

wolfram and tellurium. It is reasonably estimated that these elements accelerate the migration of lattice oxide ion and enhance the stability of catalyst.

### 3. Oxygen storage/release capacity for the automobile three way catalyst

The lean-burn engine system has been developed as a key technology to suppress the fuel consumption of vehicles. In order to reduce the emission of  $\text{NO}_x$ , CO and hydrocarbons simultaneously, the  $\text{NO}_x$  storage-reduction catalyst (NSR catalyst) was realized by Toyota group [34,35]. The effective operation of NSR catalyst also needs catalytic activities for CO, hydrocarbons and  $\text{NO}_x$  under both reducing and oxidizing conditions. Accordingly, the bank function of catalyst for oxygen gas, i.e. oxygen storage/release capacity (OSC) is also required for the three-way catalytic performance of NSR catalyst. OSC catalyst stores oxygen in the bulk of the catalyst under oxidizing conditions and uses the oxide ion stored under reducing conditions.

$\text{CeO}_2$  has been widely used for the purpose as support and co-catalyst for noble metals due to its high OSC according to the reversible redox cycle ( $2\text{CeO}_2 \rightarrow \text{Ce}_2\text{O}_3 + (1/2)\text{O}_2$ ). It has been reported that the OSC function of  $\text{CeO}_2$  is drastically improved by the effective design of the catalyst system. It was found that the addition of  $\text{ZrO}_2$  to  $\text{CeO}_2$  enhances the OSC of  $\text{CeO}_2$  and its thermal stability and the OSC of  $\text{CeO}_2$ - $\text{ZrO}_2$  catalyst strongly depends on the preparation method and resulting structure of the

Table 1  
OSC properties of  $\text{CeO}_2$ - $\text{ZrO}_2$  mixed oxides [7]

Sample	OSC <sup>a</sup> (mmol $\text{O}_2$ g cat <sup>-1</sup> )	Ce efficiency <sup>b</sup> (%)
$\text{CeO}_2$	0.05	3.0
CZ55-1	0.08	9.6
CZ55-2	0.44	51.7
CZ55-3	0.75	88.6

<sup>a</sup> OSC: oxygen storage/release capacity of 1 wt.% Pt loaded Ce compounds was measured at 773 K.

<sup>b</sup> The ratio  $\text{Ce}^{3+}/(\text{Ce}^{3+} + \text{Ce}^{4+})$  under reductive condition.

catalyst (5). Three types of  $\text{CeO}_2$ - $\text{ZrO}_2$  (CZ55-1, -2 and -3) with the same composition ( $\text{Ce}/\text{Zr} = 1$ ) were prepared by the different ways. CZ55-1 was prepared by the precipitation process using  $\text{CeO}_2$  powder with  $\text{ZrO}(\text{NO}_3)_2$  aqueous solution; CZ55-2 was by the coprecipitation from aqueous  $\text{Ce}(\text{NO}_3)_3$  and  $\text{ZrO}(\text{NO}_3)_2$  solution; CZ55-3 was by the calcination of CZ55-2 sample at  $1200^\circ\text{C}$  under reductive condition. The OSC of 1 wt.% platinum loaded  $\text{CeO}_2$ - $\text{ZrO}_2$  samples were examined at  $500^\circ\text{C}$  and the lattice oxide ion involved in the redox cycle for each sample are listed in Table 1.

As shown in Table 1, every catalyst containing  $\text{CeO}_2$  shows OSC behavior but its efficiency depends strongly on the preparation method and resulting structure. The highest OSC was obtained by CZ55-3 which shows the highest performance for cleaning automobile exhaust gases. The structure of each sample was investigated by XAFS and XRD(5). The estimated structures of CZ55-1, -2 and -3 are illustrated in Fig. 8 where only CZ55-3 forms homogeneous solid solution of  $\text{Ce}_{0.5}\text{Zr}_{0.5}\text{O}_2$ . It was concluded that

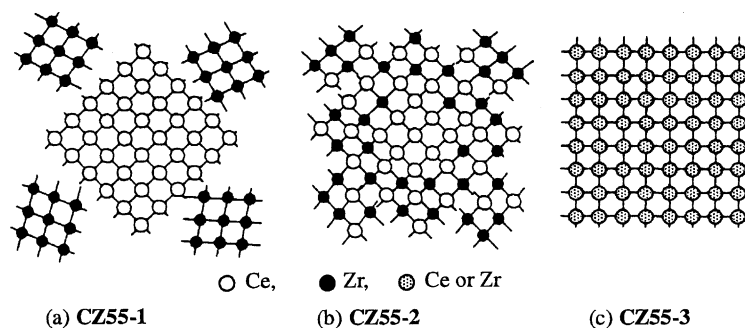


Fig. 8. Model illustration of cation-cation network for the  $\text{CeO}_2$ - $\text{ZrO}_2$  samples with the same composition ( $\text{Ce}/\text{Zr} = 1$ ). CZ55-1 consists of pure  $\text{CeO}_2$  and  $\text{ZrO}_2$ . Ce rich domain and Zr rich one in CZ55-2 still remain.  $\text{Ce}_{0.5}\text{Zr}_{0.5}\text{O}_2$  solid solution in CZ55-3 forms homogeneously at atomic level [7].



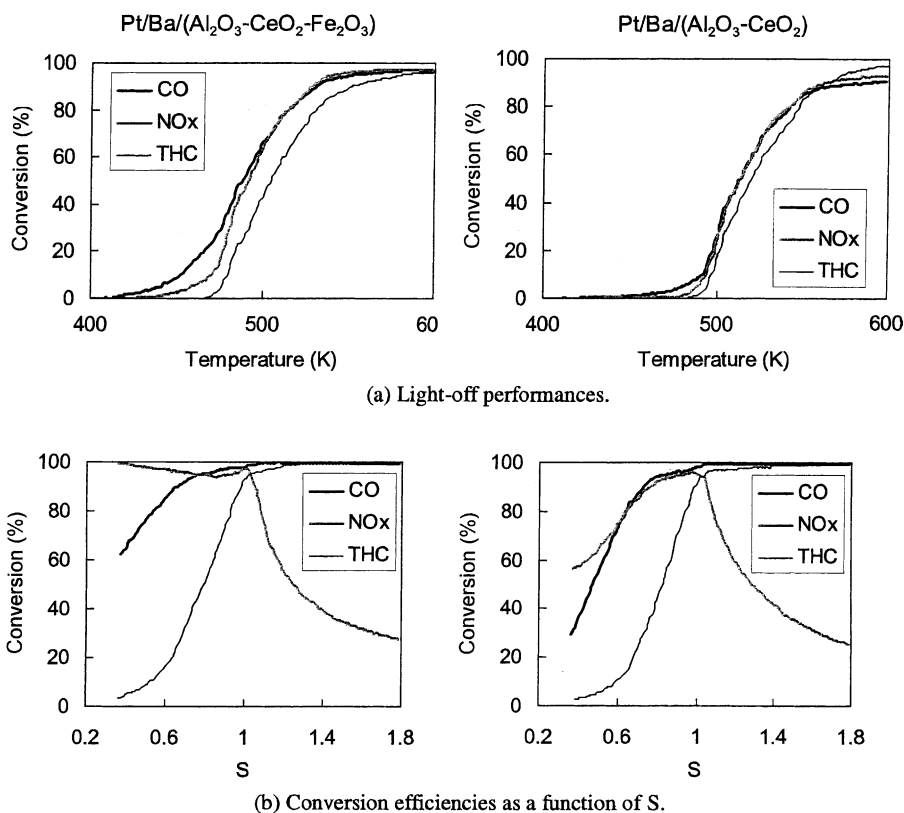


Fig. 9. The three way catalytic performance of aged Pt/Ba/(Al<sub>2</sub>O<sub>3</sub>-CeO<sub>2</sub>) with and without Fe<sub>2</sub>O<sub>3</sub>.

this structure makes a part of metal–oxygen bond weaken and enhances the OSC of catalyst. The reason was mainly attributed to thermodynamical aspect. This important principle for the design of practical automobile catalyst is still under investigation and kinetic investigations including the migration of oxide ion may be desired to understand the whole results completely.

The three way catalytic performance of NSR catalysts under stoichiometric conditions, especially after thermal aging, was also investigated by Toyota group and improved results were understood by the OSC of catalysts [8]. It was found that the three way catalytic activity of Pt/Ba/(Al<sub>2</sub>O<sub>3</sub>-CeO<sub>2</sub>) catalyst after aging was improved by the addition of Fe<sub>2</sub>O<sub>3</sub>.

Although the fresh catalysts show almost the same performance with or without Fe<sub>2</sub>O<sub>3</sub>, the catalytic activity of the aged catalyst without Fe<sub>2</sub>O<sub>3</sub> was poor as shown in Fig. 9. The reason is attributable to the dif-

ference of the OSC of two catalysts as presented in Fig. 10. Thus, the oxygen bank function of oxide catalyst has been successfully applied to the design of practical industrial catalysts.

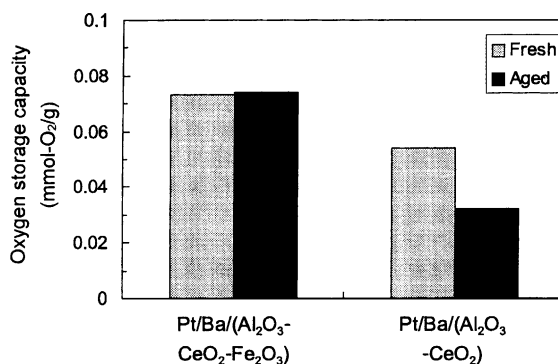


Fig. 10. Oxygen storage capacity of Pt/Ba/(Al<sub>2</sub>O<sub>3</sub>-CeO<sub>2</sub>) with and without Fe<sub>2</sub>O<sub>3</sub>.

#### 4. Conclusion

The participation of lattice oxide ion has been sporadically reported in the catalytic oxidation over metal oxide catalysts. By the systematic investigation using  $^{18}\text{O}$  tracer, it has been demonstrated that excellent industrial metal oxide catalysts have been often developed by the skillful utilization of this phenomenon. The concept of oxygen bank function including rapid migration of oxide ion through bulk diffusion has been established and it is expected to be widely employed for the design of excellent industrial oxidation catalysts.

#### References

- [1] P. Mars, D.W. van Krevelen, Chem. Eng. Sci. (Special Suppl.) 3 (1954) 41.
- [2] G.W. Keulks, J. Catal. 19 (1970) 232.
- [3] R.D. Wragg, P.G. Ashmore, J.A. Hockey, J. Catal. 22 (1971) 49.
- [4] R.D. Wragg, P.G. Ashmore, J.A. Hockey, J. Catal. 28 (1973) 331.
- [5] Y. Moro-oka, W. Ueda, Adv. Catal. 40 (1994) 233.
- [6] W. Ueda, C.-L. Chen, K. Asakawa, Y. Moro-oka, T. Ikawa, J. Catal. 101 (1986) 369.
- [7] Y. Nagai, T. Yamamoto, T. Tanaka, S. Yoshida, T. Nonaka, T. Okamoto, A. Suda, M. Sugiura, in: Proceedings of the 8th Japan–Korea Symposium on Catalysis, 2001, p. 57.
- [8] K. Yamazaki, N. Takahashi, H. Shinjo, M. Sugiura, in: Proceedings of the 8th Japan–Korea Symposium on Catalysis, 2001, p. 135.
- [9] N. Kominami, Kogyo Kagaku Zasshi 65 (1962) 1510.
- [10] J.D. Idol, US Patent 2,904,580, Standard Oil Co., Ohio (1959).
- [11] F. Veatch, J.L. Callahan, F.C. Milberger, R.W. Formane, in: Proceedings of the 2nd International Congress on Catalysis, vol. 2, Technip, Paris, 1961, p. 2674.
- [12] F. Veatch, J.L. Callahan, J.D. Idol, E.C. Milberger, Hydrocarbon Process, Pet. Refiner 41 (1962) 187.
- [13] R.K. Grasselli, J.D. Burrington, Adv. Catal. 30 (1981) 133.
- [14] Dutch Patent 1,125,901 Knapsack A.G. (1962).
- [15] German Patent 1,234,175 (1967).
- [16] S. Takenaka, G. Yamaguchi, Japanese Kokai JP 43/002,324 (1968), JP 44/005,855 (1969), JP 44/006,264 (1969), Nippon Kayaku Co.
- [17] T. Sasaki, Y. Nakamura, K. Moritani, A. Morii, S. Saito, Shokubai 14 (1972) 191, and references therein.
- [18] A.W. Sleight, W. Jeitschko, Mater. Res. Bull. 9 (1974) 951.
- [19] T. Notermann, G.W. Keulks, A. Skliarov, Yu. Maximov, L.Ya. Margolis, O.V. Krylov, J. Catal. 39 (1975) 266.
- [20] M. Lajcono, T. Motermann, G.W. Keulks, J. Catal. 40 (1975) 19.
- [21] W. Ueda, Y. Moro-oka, T. Ikawa, I. Matsuura, Chem. Lett. (1982) 1365.
- [22] Y. Moro-oka, D.-H. He, W. Ueda, Stud. Surf. Sci. Catal. 67 (1991) 57.
- [23] Y.H. Han, W. Ueda, Y. Moro-oka, Appl. Catal. A 176 (1991) 11.
- [24] H. Ponceblanc, J.M.M. Millet, G. Coudurier, J.M. Herrmann, J.C. Vedrine, J. Catal. 142 (1993) 373, 381.
- [25] H. Hashiba, M. Kanesaka, I. Matsuura, Shokubai 27 (1985) 434.
- [26] W. Ueda, K. Asakawa, C.-L. Chen, Y. Moro-oka, T. Ikawa, Catalysis 101 (1986) 360.
- [27] J.D. Bierlein, A.W. Sleight, Solid State Commun. 16 (1975) 69.
- [28] K. Aykan, A.W. Sleight, D.B. Rogers, J. Catal. 29 (1973) 185.
- [29] K. Aykan, D. Halvorson, A.W. Sleight, D.B. Rogers, J. Catal. 35 (1974) 401.
- [30] W.J. Linn, A.W. Sleight, J. Catal. 41 (1976) 134.
- [31] A.W. Sleight, K. Aykan, D.B. Rogers, J. Solid State Chem. 13 (1975) 231.
- [32] E.V. Howfs, J.R. Monnier, G.W. Keulks, J. Catal. 57 (1979) 331.
- [33] Y. Moro-oka, W. Ueda, Shokubai 25 (1983) 271, and references therein.
- [34] N. Takahashi, H. Shinjo, T. Iijima, T. Suzuki, K. Yamazaki, K. Yokota, H. Suzuki, N. Miyoshi, S. Matsumoto, T. Tanizawa, T. Tanaka, S. Tateishi, K. Kasahara, Catal. Today 27 (1996) 63.
- [35] K. Yamazaki, T. Suzuki, N. Takahashi, K. Yokota, M. Sugiura, Appl. Catal. B 30 (2001) 459.